## Title

Secretagogin is Expressed by Developing Neocortical GABAergic Neurons in Humans but not Mice and Increases Neurite Arbor Size and Complexity.



## Journal

Cerebral cortex (New York, N.Y. : 1991), 28(6)

## ISSN

1047-3211

## Authors

Raju, Chandrasekhar S
Spatazza, Julien
Stanco, Amelia
et al.

## Publication Date

2018-06-01

## DOI

10.1093/cercor/bhx101

Peer reviewed

*Cerebral Cortex*, 2017; 1–13

**doi: 10.1093/cercor/bhx101**
Original Article

ORIGINAL ARTICLE

# Secretagogin is Expressed by Developing Neocortical GABAergic Neurons in Humans but not Mice and Increases Neurite Arbor Size and Complexity

Chandrasekhar S. Raju[1,2], Julien Spatazza[1,2,7], Amelia Stanco[3,8], Phillip Larimer[4,5], Shawn F. Sorrells[1,2], Kevin W. Kelley[1,2], Cory R. Nicholas[2,5,7], Mercedes F. Paredes[2,5], Jan H. Lui[2,5,9], Andrea R. Hasenstaub[4,6], Arnold R. Kriegstein[2,5], Arturo Alvarez-Buylla[1,2], John L. Rubenstein[3] and Michael C. Oldham[1,2]

[1]Department of Neurological Surgery, University of California, San Francisco, USA, [2]The Eli and Edythe Broad Center of Regeneration Medicine and Stem Cell Research, University of California, San Francisco, USA, [3]Department of Psychiatry, University of California, San Francisco, USA, [4]Center for Integrative Neuroscience, University of California, San Francisco, USA, [5]Department of Neurology, University of California, San Francisco, USA, [6]Department of Otolaryngology-Head and Neck Surgery, University of California, San Francisco, USA, [7]Present address: Neurona Therapeutics, South San Francisco, CA, USA, [8]Present address: EntroGen, Woodland Hills, CA, USA and [9]Present address: Howard Hughes Medical Institute and Department of Biology, Stanford University, Stanford, CA, USA

Address correspondence to Michael C. Oldham. Email: Michael.Oldham@ucsf.edu

## Abstract

The neocortex of primates, including humans, contains more abundant and diverse inhibitory neurons compared with rodents, but the molecular foundations of these observations are unknown. Through integrative gene coexpression analysis, we determined a consensus transcriptional profile of GABAergic neurons in mid-gestation human neocortex. By comparing this profile to genes expressed in GABAergic neurons purified from neonatal mouse neocortex, we identified conserved and distinct aspects of gene expression in these cells between the species. We show here that the calcium-binding protein secretagogin (SCGN) is robustly expressed by neocortical GABAergic neurons derived from caudal ganglionic eminences (CGE) and lateral ganglionic eminences during human but not mouse brain development. Through electrophysiological and morphometric analyses, we examined the effects of *SCGN* expression on GABAergic neuron function and form. Forced expression of *SCGN* in CGE-derived mouse GABAergic neurons significantly increased total neurite length and arbor complexity following transplantation into mouse neocortex, revealing a molecular pathway that contributes to morphological differences in these cells between rodents and primates.

**Key words:** gene coexpression, human brain development, interneurons, neuronal maturation, species differences

## Introduction

Ramón y Cajal surmised a century ago that the unusual cognitive abilities of humans were related to the functions of neocortical neurons with "short axons" (Cajal 1923), which are known today as interneurons. Based on qualitative analysis of hundreds of tissue sections using Golgi's silver impregnation technique, he proposed that interneurons are more abundant and morphologically diverse in primate neocortex (and particularly, human neocortex) compared with neocortices of rodents and other mammals. Neocortical interneurons include spiny non-pyramidal cells, which are mostly excitatory and located in layer IV, and aspiny non-pyramidal cells, which are inhibitory (GABAergic) and distributed throughout the cortical wall (Jones and Peters 1984; DeFelipe et al. 2013). Modern estimates indicate that GABAergic neurons comprise ~15% of all neocortical neurons in rats and mice and >20% in monkeys and humans (Lin et al. 1986; Fitzpatrick et al. 1987; Hendry et al. 1987; Meinecke and Peters 1987; Beaulieu et al. 1992, 1994; Ren et al. 1992; Beaulieu 1993; Hornung and De Tribolet 1994; Jones et al. 1994; Micheva and Beaulieu 1995; del Rio and DeFelipe 1996; Gabbott and Bacon 1996; Gabbott et al. 1997; Tamamaki et al. 2003; Santana et al. 2004; Dzaja et al. 2014). The proportion is even higher in superficial layers of human neocortex, where nearly 40% of neurons in some regions are GABAergic (del Rio and DeFelipe 1996).

The increase in the proportion of GABAergic neurons in primate neocortex is thought to primarily reflect an increase in the vasoactive intestinal polypeptide (VIP)/calretinin (CR)-expressing subtype (Hansen et al. 2013; Dzaja et al. 2014; Hladnik et al. 2014; Barinka et al. 2015), which arises in the caudal and lateral ganglionic eminences (CGE/LGE) and preferentially occupies superficial cortical layers (Xu et al. 2004; Fogarty et al. 2007; Miyoshi et al. 2010). In humans, half or more of neocortical GABAergic neurons may derive from the CGE (Hansen et al. 2013), whereas in mice this number is closer to ~30% (Miyoshi et al. 2010). In addition to these quantitative differences, CGE/LGE-derived neocortical GABAergic neurons also differ morphologically between primates and rodents. In the adult primate neocortex, $VIP^+/CR^+$ GABAergic neurons often exhibit a "horse-tail" morphology (a term that encompasses bitufted, bipolar, and double-bouquet cells) (DeFelipe et al. 2013). These cells are characterized by long, vertically oriented axon collaterals that can form hundreds of inhibitory synapses with dendrites of pyramidal cells from several cortical layers (Cajal 1899; DeFelipe et al. 2006). This unique morphology is not evident in rodents but is thought to play a critical role in the microcolumnar organization of neocortical circuits in primates (Yanez et al. 2005; DeFelipe et al. 2006; Jones 2009).

Because CGE/LGE-derived, $VIP^+/CR^+$ GABAergic neurons are present in rodent neocortex, these observations suggest that horse-tail neurons in primates represent an elaboration of an existing cell type (as opposed to wholesale creation of a novel cell type; Hansen et al. 2013). However, there is no molecular explanation for morphological differences in $VIP^+/CR^+$ neocortical GABAergic neurons between rodents and primates. Indeed, although several studies have examined the origins and development of human GABAergic neurons (Bayatti et al. 2008; Jakovcevski et al. 2011; Radonjic et al. 2014b; Al-Jaberi et al. 2015), to our knowledge, no molecular differences between GABAergic neurons of rodents and primates have been described. Given the increasing appreciation for the role of GABAergic dysfunction in a variety of human neurodevelopmental disorders (Marin 2012; Southwell et al. 2014), it is critical to understand the molecular bases of GABAergic neuron specification and maturation in the human brain (Clowry et al. 2010; Molnar and Clowry 2012). We therefore set out to determine the extent to which transcriptional programs are conserved in nascent neocortical GABAergic neurons between humans and mice.

## Materials and Methods

### Tissue Collection and Processing

#### *Human*

Prenatal human brain samples were collected and processed as previously described (Lui et al. 2014). Samples were obtained from elective pregnancy terminations at San Francisco General Hospital, usually within 2 h of the procedure. Donated human tissues were examined only from patients who had previously given informed consent and in strict observance of state and institutional legal and ethical requirements. Research protocols were approved by the Human Gamete, Embryo, and Stem Cell Research Committee (institutional review board) at the University of California, San Francisco (UCSF). Gestational age was determined using foot length. Tissues were transported in Leibowitz-15 medium on ice to the laboratory. The gestational week 18 (GW18) neocortical sample analyzed by Gene Coexpression Analysis of Serial Sections (GCASS) was frozen rapidly on dry ice and stored at −80 °C prior to cryosectioning. Cryosections ($n$ = 120) were cut along the longest axis of the

**Table 1** Human brain samples analyzed in this study

| Source | Method | No. samples | No. individuals | Age(s) | Enrichment P-value* | Relevant figure(s) |
|---|---|---|---|---|---|---|
| Johnson et al. (2009) | Microarray (AffyExon1.0) | 30 | 2 | 18–19 GW | $3.68\times10^{-13}$ | 1 |
| Miller et al. (2014) | Microarray (Agilent) | 167 | 1 | 18 GW | $2.89\times10^{-27}$ | 1 |
| brainspan.org | RNA-seq | 37 | 4 | 17–19 GW | $3.95\times10^{-7}$ | 1 |
| This study | Microarray (ILMNHT12v4) | 87 | 1 | 18 GW | $1.96\times10^{-20}$ | 1, S1, S2 |
| This study | Immunostain | 14 | 7 | 14.5 GW<br>18 GW<br>Birth<br>7 months<br>6 years<br>24 years | NA | 2–4, S2, S3, S5, S6, S9 |
| This study | Cell culture | 3 | 1 | 15 GW | NA | S7 |

GW, gestational weeks; Affy, Affymetrix; ILMN, Illumina. *The most significant P-value (one-sided Fisher's exact test) for enrichment of a set of human interneuron markers (Zeng et al. 2012) in a gene coexpression module from each analyzed microarray / RNA-seq data set.

tissue specimen at 150 μm section thickness, collected in individual Eppendorf tubes, and immediately transferred to dry ice and stored at −80 °C to prevent RNA degradation.

For immunostaining, prenatal tissue samples were fixed overnight at 4 °C in 4% paraformaldehyde (PFA) in phosphate-buffered saline (PBS), cryoprotected in 30% sucrose in PBS at 4 °C, embedded and frozen in O.C.T. compound (Tissue-Tek, Inc.) at −80 °C, and sectioned on a Leica CM3050S cryostat (10–20 μm thick) onto glass slides, which were stored at −80 °C. Total postmortem interval was typically 3–4 h before fixation. Postnatal tissue samples were obtained at autopsy with postmortem intervals ≤48 h. Causes of death were pneumonia (7-month case), lung hypoplasia (6-year case), and hepatic failure/Crohn's disease (24-year case). Brains were cut into 1.5 cm coronal blocks, fixed in 4% PFA for 48 h, cryoprotected in 30% sucrose in PBS at 4 °C, and embedded and frozen in O.C.T. compound (Tissue-Tek, Inc.) at −80 °C. Blocks were sectioned on a Leica CM3050S cryostat (20–30 μm thick) onto glass slides, which were stored at −80 °C. A summary of all human samples analyzed in this study is presented below in Table 1.

#### *Mouse*

All protocols and procedures followed UCSF guidelines and were approved by the UCSF Institutional Animal Care and Use Committee. *Vip-Cre;R26-Ai14* and wild-type C57BL/6 J breeders were purchased from the Jackson Laboratory (https://www.jax.org). Pregnant mice were anesthetized with Avertin and embryonic brains were dissected and fixed overnight at 4 °C in 4% PFA in PBS. Brains were cryoprotected for at least 24 h in 30% sucrose in PBS at 4 °C, then embedded and frozen in O.C.T. compound (Tissue-Tek, Inc.).

### Fluorescent-Activated Cell Sorting

For fluorescent-activated cell sorting (FACS) of mouse GABAergic neurons, neocortices of 4 P0 *Cxcr7-Gfp* mice were dissected in cold Hank's Balanced Salt Solution (HBSS) and treated with 0.25% trypsin and DNase I at 37 °C for 15 min. Following this treatment, the trypsin/DNase I solution was replaced with DMEM/10% fetal bovine serum and the tissue was mechanically dissociated through repeated pipetting. Cells were pelleted by centrifugation and the supernatant was replaced with 500 μL of HBSS with propidium iodide (PI). After another round of trituration, cells from each neocortex were passed through a 35 μm filter immediately prior to FACS, which was performed using a BD FACSAria II cell sorter (BD Biosciences). GFP-negative neocortices served as a control for fluorescence. Collection windows were set to obtain $GFP^+/PI^-$ cells, yielding ~50 000 cells/neocortex.

### RNA Extraction and Quality Control

#### *Human*

For the GCASS data set, total RNA was extracted from each cryosection ($n$ = 120) of GW18 neocortex using the miRNeasy Mini kit on a QIAcube automated sample preparation system according to the manufacturer's instructions (Qiagen, Inc.). Total RNA quantity and quality were assessed using a Nanodrop ND-8000 (Nanodrop Technologies, Inc.) and a Bioanalyzer 2100 (Agilent Technologies, Inc.), respectively. The average yield of total RNA/section over all sections was ~966 ng. Samples were evaluated on the basis of RNA yield, 260/280 and 260/230 nm absorption ratios, and RNA integrity (RIN) scores. RNA samples ($n$ = 94) were selected for microarray analysis per the following criteria: 260/280 > 2, 260/230 > 1 (with ~80% of sections having 260/230 > 1.6), and RIN > 9.

#### *Mouse*

Following FACS, ~50 000 *Cxcr7-Gfp*$^+$ cells/neocortex were immediately processed for RNA extraction using the RNeasy micro kit (Qiagen, Inc.). Total RNA quantity and quality were assessed using a Nanodrop ND-8000 (Nanodrop Technologies, Inc.) and the Pico Chip on a Bioanalyzer 2100 (Agilent Technologies, Inc.), respectively.

### Microarray Data Generation and Processing

#### *Human*

For the GCASS data set, total RNA from 94 high-quality samples was shipped on dry ice to the University of California, Los Angeles (UCLA) Neurogenomics Core facility for analysis using Illumina HT-12 v4 human microarrays (Illumina, Inc.). The order of the samples was randomized prior to shipment to avoid confounding potential technical artifacts with potential biological gradients of gene expression. Two control samples from the same pool of total human brain RNA (Ambion FirstChoice human brain reference RNA Cat#AM6050, Life Technologies, Inc.) were included to facilitate microarray data preprocessing. All 96 samples were processed in the same batch for amplification (Ambion/Illumina TotalPrep RNA Amplification kit), labeling, and hybridization. Bead-level raw data were minimally processed by the UCLA Neurogenomics core facility (no normalization or background correction) using BeadStudio software (Illumina, Inc.). Microarray data have been deposited in Gene Expression Omnibus (http://www.ncbi.nlm.nih.gov/geo/) under accession ID GSE95639.

Minimally processed microarray expression data were further preprocessed using the SampleNetwork R function (Oldham et al. 2012), which is designed to identify and remove outlying samples, perform data normalization (Bolstad et al. 2003), and adjust for batch effects (Johnson et al. 2007). Briefly, application of SampleNetwork to the GCASS data set revealed 3 distinguishing features. First, sample homogeneity was extremely high, as evidenced by the mean inter-sample adjacency and the correlation between the standardized sample connectivity and clustering coefficient (cor($k$,$C$)). Second, despite the high overall level of sample homogeneity, 7 outlier samples were identified ($Z.K < -3$) and excluded prior to quantile normalization (Bolstad et al. 2003). Third, following quantile normalization there remained a significant batch effect associated with array ID (each Illumina HT-12 v4 microarray analyzes 12 samples in parallel), which was corrected by ComBat normalization (Johnson et al. 2007).

#### *Mouse*

Total RNA from ~200 000 FACS-sorted *Cxcr7-Gfp*$^+$ cells was pooled and amplified using the Complete Whole Transcriptome Amplification kit according to manufacturer's instructions (Sigma-Aldrich, Inc.). Cy3-CTP labeling was performed using NimbleGen one-color labeling kits (Roche-NimbleGen, Inc.). Labeled target was quantified with the Nanodrop ND-8000 (Nanodrop Technologies, Inc.) and equal amounts of Cy3-labeled target were hybridized to Agilent whole mouse genome 4×44 K ink-jet microarrays (Agilent, Inc.). Hybridizations were performed for 17 h, according to the manufacturer's protocol. Microarrays were scanned using the Agilent microarray scanner and raw signal intensities were extracted with Feature Extraction v10.1 software. No background subtraction was

performed, and the median feature pixel intensity was used as the raw signal before quantile normalization (Bolstad et al. 2003).

## Gene Coexpression Module Detection and Integration

Gene coexpression analysis was performed in the R computing environment (R; http://cran.us.r-project.org). For the GCASS data set, gene coexpression analysis was restricted to 30 425 probes that were re-annotated as either "perfect" (the probe uniquely and perfectly matches the target transcript; $n$ = 29 272) or "good" (the probe matches the target transcript with up to 2 mismatches; $n$ = 1153) (Barbosa-Morais et al. 2010). Gene coexpression modules were identified as previously described (Lui et al. 2014) using a 4-step approach. First, pairwise biweight midcorrelations (bicor) were calculated among 30 425 transcripts across all 87 samples using the WGCNA R package (Langfelder and Horvath 2008). Second, transcripts were clustered using the flashClust (Langfelder and Horvath 2008) implementation of a hierarchical clustering procedure with complete linkage and 1—bicor as a distance measure. The resulting dendrogram was cut at a series of static heights, corresponding to the top X% of values in the entire data set (where X = 0.01%, 0.1%, 1%, 2%, 3%). Third, all clusters consisting of at least Y members (where Y = 8, 10, 12, 15, 20) were identified and summarized by their module eigengene (i.e., the first principal component obtained by singular value decomposition) using the moduleEigengenes function of the WGCNA R package (Langfelder and Horvath 2008). Fourth, highly similar modules were merged if the Pearson correlations of their module eigengenes exceeded an arbitrary threshold (0.85). This procedure was performed iteratively such that the pair of modules with the highest correlation >0.85 was merged, followed by recalculation of all module eigengenes, followed by recalculation of all correlations, until no pairs of modules exceeded the threshold. Following these steps, a series of 25 coexpression networks were constructed, each consisting of zero to several hundred coexpression modules. For each network, the WGCNA measure of intramodular connectivity ($k_{ME}$) was calculated for all probes (47 231) with respect to all modules by correlating each probe's expression pattern across all 87 samples with each module eigengene.

To identify a gene coexpression module corresponding to nascent GABAergic neurons, we cross-referenced all modules from all 25 coexpression networks with a set of genes whose expression marks human GABAergic neurons (Zeng et al. 2012) (using gene symbol as a common identifier). Modules were defined as consisting of all unique genes that were positively and specifically correlated with the module eigengene at a significance threshold corresponding to a Bonferroni-corrected $P$-value (0.05 / [47 231 probes × the number of coexpression modules in the network]). The statistical significance of module enrichment was determined using a one-sided Fisher's exact test as implemented by the fisher.test R function. The module with the most significant enrichment ($P = 1.96\times10^{-20}$) was found in a network consisting of 10 modules (corresponding to network construction parameters of X = 0.1% and Y = 15). The same strategy was used to identify gene coexpression signatures of GABAergic neurons in additional prenatal human brain gene expression data sets (Johnson et al. 2009; Miller et al. 2014) (Table 1).

Note that data from Miller et al. (2014) correspond to individual H376.IIIB.02. For each of these data sets, quality control was performed with the SampleNetwork R function (Oldham et al. 2012), a series of unsupervised gene coexpression networks was constructed, and the module with the most significant enrichment of human GABAergic neuron markers in each data set was identified (Zeng et al. 2012), as described above (see Table 1 for enrichment $P$-values for the most significant module in each data set). The expression patterns of these modules were summarized by their module eigengenes and the WGCNA measure of intramodular connectivity, $k_{ME}$, was calculated for all probes/genes in each data set by correlating their expression patterns over all samples with the GABAergic neuron module eigengene (Langfelder and Horvath 2008). To aggregate $k_{ME}$ values across the 4 studies, we used Fisher's method for combining correlation coefficients from independent data sets (Fisher 1970). The resulting metric summarizes expression fidelity for GABAergic neurons in prenatal human neocortex as a z-score.

## Immunostaining

For immunostaining, cryosections were thawed in PBS and subjected to heat-induced antigen retrieval in 0.01 M sodium citrate (pH 6.0) for 10 min. Sections were incubated with blocking buffer (10% normal donkey or goat serum in PBS, with 0.2% Triton X-100) for 1 h at room temperature. Primary and secondary antibodies were diluted in blocking buffer. First, sections were incubated with primary antibodies overnight at 4 °C in a humidified chamber. Sections were then incubated with secondary antibodies and DAPI (4′,6-diamidino-2-phenylindole) for 60–90 min at room temperature. Both primary and secondary stains were washed extensively in PBS plus 0.2% Triton X-100 to reduce nonspecific binding of antibodies. Slides were mounted with fluorogel mounting medium (Electron Microscopy Sciences, Inc.). The following primary antibodies were used: SP8 (1:1000, goat, Santa Cruz Biotech, Inc.), SCGN (1:1000, rabbit, Sigma-Aldrich, Inc.), SCGN (1:500, mouse, Sigma-Aldrich, Inc.), GABA (1:1000, rabbit, Sigma-Aldrich, Inc.), DCX (1:500, Guinea pig, Millipore, Inc.), CALB2 (CR) (1:2000, mouse, Swant, Inc.), TBR1 (1:500, guinea pig, Labome, Inc.), TBR2 (1:1000, chicken, EMD Millipore, Inc.), Ki-67 (1:200, mouse, BD Biosciences, Inc.), COUP-TFII (1:1000, mouse, Perseus Proteomics, Inc.), NKX2.1 (1:200, mouse, Novocastra, TTF1), VIP (1:200, mouse, R&D Systems, Inc.), GFP (1:2000, chicken, Abcam), and tdTomato (1:2000, rat, ChromoTek). Species-specific fluorophore-conjugated secondary antibodies Alexa Fluor 488, Alexa Fluor 546, and Alexa Fluor 647 were obtained from Thermo Fisher Scientific, Inc. and used according to manufacturer's instructions. For doublecortin (DCX) detection, tyramide signal amplification (Perkin-Elmer, Inc.) was performed according to manufacturer's instructions. Briefly, sections were incubated with the biotinylated secondary antibody (1:500, Jackson Immunoresearch Laboratories, Inc.) for 2.5 h at room temperature and for 30 min in streptavidin–horseradish peroxidase that was diluted (1:200) in blocking buffer. Sections were then incubated in tyramide-conjugated fluorophores (Fluorescein, 1:50) for 5 min.

## Confocal Imaging and Cell Counting

All of the images in this study were acquired on Leica TCS SP5 laser confocal microscopes. Images were acquired in Tilescan mode with automatic stitching of arrayed tiles using either 10× lens with 1.5–2.0× optical zoom or 20× lens with 1.0× optical zoom, and confocal $z$-stacks of optical sections were displayed as maximum intensity projections. For cell counting, confocally imaged data files were opened with Imaris imaging software (Bitplane, Inc.) for colocalization analyses. Colocalization

counts were performed essentially as described (Hansen et al. 2010). For quantification of neocortical GABAergic neurons, three 20 μm coronal sections sampled at 200 μm intervals were analyzed. Counting regions in each section spanned the entire cortical wall, from the ventricular zone to the pial surface, with a width of 500 μm. Fluorescence signals from immunoreactivity for SP8/CR/N2F2 and SCGN were first counted separately using the "spots" function in Imaris imaging software. A threshold for mean intensity was selected to identify fluorescent spots with a 5 μm diameter in each channel as a representation of the number of cells. The preliminary sets of positive cells were then manually edited to correct software error. Double-colocalized spots were then calculated by MATLAB (Mathworks, Inc.) and the ImarisXT module, and further edited to correct software errors. The numbers of colocalized spots were recorded.

## Cell Culture

The ventricular and subventricular layers of the medial ganglionic eminence (MGE), LGE, and CGE were dissected from GW15 ventral telencephalon. Explants were mechanically dissociated in Leibovitz L-15 medium containing DNase I (100 μg $mL^{-1}$) into a single-cell suspension by repeated pipetting. Dissociated cells were centrifuged (3 min at 1000*g*), resuspended, and cultured in neurobasal medium supplemented with B27 (Gibco, Inc.; Thermo Fisher Scientific, Inc.) on Matrigel Matrix. Approximately 200 000 cells were plated per well in a 24-well plate. Cultures were fed twice weekly by replacing half of the medium. After 4 weeks, cells were fixed in 4% PFA, permeabilized with 0.2% triton-100, and triple immunostained for NKX2.1, SP8, and SCGN.

## Cloning and Lentivirus Production

Total RNA was extracted from GW18 prenatal human neocortex and cDNA synthesis was performed using SuperScript III Reverse Transcriptase (Thermo Fisher Scientific, Inc.). Full-length human *SCGN* was cloned into a pSLIC-GfpP2A lentiviral plasmid (ATGCbio, Inc.) using the following primers:

- Forward primer: AACCCTGGACCTGATGACAGCTCCCGGGAACCGA
- Reverse primer: GCCACTGTGCTGGATAGAGCAAAAGGCAAAGCAGTC

Constructs were verified by Sanger sequencing. Lentiviral preparation and concentration was performed at the UCSF VIRACORE facility.

## Viral-Mediated Labeling and Transplantation of CGE Cells

*Vip-Cre* and *R26-Ai14* mice were purchased from the Jackson Laboratory (http://www.jax.org). The ventricular and subventricular zones of E14.5 CGE were dissected from donor embryos and dissociated by repeated pipetting in Leibovitz's L-15 medium containing 100 U/mL DNase I (Roche, Inc.). Dissociated cells were incubated with concentrated lenti-*Gfp* or lenti-*Gfp-SCGN* virus for 30 min in neurobasal medium supplemented with B27 (Gibco, Inc.; Thermo Fisher Scientific, Inc.) at 37 °C in an incubator. After incubation with lentivirus, the supernatant was removed, and cells were washed 3 times and concentrated via centrifugation (800*g* for 3 min). P2 recipient mice were anesthetized via hypothermia until pedal reflex disappeared and then placed on a stereotaxic platform for injection of concentrated cells (~300 cells/nL × 200 nL/injection ≈ 60k cells/injection) through a beveled Drummond glass micropipette (Drummond Scientific, Inc.) positioned at 30° from vertical. Two injections were placed into the caudal left cortex at 7 mm posterior/3.5 mm lateral and 6.5 mm posterior/3.2 mm lateral, as measured from the inner corner of the eye (for anterior zero) and the midpoint between the 2 eyes (for midline zero), resulting in ~120 k injected cells/animal. Injections were made at 0.8–1.2 mm deep from the skin surface. After injection, recipients were placed on a heating pad until warm and active at which time they were returned to their mothers until weaning (P21).

## Slice Preparation and Electrophysiology

Slice preparation and electrophysiology were performed as described (Larimer et al. 2016). Briefly, transplantation was performed at P2 and slices of host brains were prepared at P50. Animals were overdosed with pentobarbital, decapitated, and the brain was removed into ice-cold dissection buffer containing (in mM): 234 sucrose, 2.5 KCl, 10 $MgSO_4$, 1.25 $NaH_2PO_4$, 24 $NaHCO_3$, 11 dextrose, 0.5 $CaCl_2$, bubbled with 95% $O_2$/5% $CO_2$ to a pH of 7.4. Coronal slices of cortex (300 μm) were prepared with a vibratome and transferred to a holding chamber filled with artificial cerebrospinal fluid containing (in mM): 124 NaCl, 3 KCl, 2 $MgSO_4$, 1.23 $NaH_2PO_4$, 26 $NaHCO_3$, 10 dextrose, 2 $CaCl_2$ (bubbled with 95% $O_2$/5% $CO_2$) and incubated at 33 °C for 30 min then stored at room temperature until slices were transferred to a flow chamber for recording. Transplanted VIP-expressing neurons were identified by their red fluorescence (red) with those that were infected with lentiviral constructs also having green fluorescence. Labeled cells were mostly found in layers II/III. Impact of viral infection (green) and consequent *SCGN* expression (gold) on intrinsic physiological properties were assessed using injection of 500 ms current pulses through a recording pipette in whole-cell configuration and an intracellular solution that contained (in mM): 140 K gluconate, 2 $MgCl_2$, 10 HEPES, 0.2 EGTA, 4MgATP, 0.3 NaGTP, 10 phosphocreatine (290 mOsm, pH 7.3), and 0.1 Alexa680.

## Morphometric Analysis of Neurite Length and Arborization

Three hundred micrometer coronal slices of neocortex were fixed with 4% PFA and immunostained for 48 h at 4 °C. Confocal images of isolated individual $tdTomato^+$ $GFP^+$ $SCGN^-$ cells ($n$ = 21 from 4 animals) and $tdTomato^+$ $GFP^+$ $SCGN^+$ cells ($n$ = 20 from 4 animals) were collected using a 20× objective on a Leica TCS SP5 microscope. Many labeled cells were seen around the injection site, but these were difficult to quantify morphometrically due to extensive overlap among neuronal arbors. We therefore focused on neurons that could be unambiguously resolved for morphometric analysis, which tended to include cells that had migrated away from the injection sites. Among these cells, we did not observe a significant relationship between laminar position or distance from the injection site and morphometric features. 70–100 μm z-stacks were collected with a step size of 2 μm and imported into Neurolucida software (MBF bioscience, Inc.) for neurite arbor tracing in 3-D. The Sholl analysis function of Neurolucida explorer was used to draw concentric spheres at 10 μm radius intervals from the

soma. Total neurite length and the number of branches (node points) per neuron were summarized from the Sholl analysis.

## Results

### Identification of a Consensus Transcriptional Profile of GABAergic Neurons in Mid-Gestation Human Neocortex and Comparison with Mice

To identify genes expressed by nascent GABAergic neurons in humans, we analyzed a single neocortical specimen from GW18 using a strategy called GCASS (Fig. 1A, Supplementary Fig. 1A), which exploits variation in cellular abundance across serial sections to reveal patterns of transcriptional covariation driven by individual cell types (Lui et al. 2014). We performed unsupervised gene coexpression analysis of microarray data from 87 sections and identified 10 modules of genes with distinct patterns of transcriptional covariation (Supplementary Fig. 1B). Unbiased enrichment analysis revealed that one module (green) was significantly enriched with markers of human GABAergic neurons (Zeng et al. 2012) ($P = 1.96\times10^{-20}$; Supplementary Fig. 1C). We summarized the expression pattern of this module by its first principal component, or module eigengene (Supplementary Fig. 1D), and calculated the extent to which each microarray probe ($n = 47\,231$) conformed to this pattern, or $k_{ME}$ (Langfelder and Horvath 2008; Oldham et al. 2008). The mRNA targets of the top 15 probes ranked by $k_{ME}$ included *DLX1*, *DLX5*, *LHX6*, *GAD2*, *CALB2* (*CR*), *GAD1*, and *SLC32A1* (*VGAT*) (Fig. 1B). These results indicate that transcriptional covariation in the green module is primarily driven by gene coexpression in nascent GABAergic neurons of the developing human neocortex. Interestingly, this module was also significantly enriched with genes located near human accelerated regions of the genome ($P = 4.63\times10^{-08}$), including *ARX*, *BHLHB2*, *CERK*, *ELAVL4*, *MAF*, *NPAS3*, *NXPH1*, *PLXNC1*, *SH3BP4*, and *ZBTB16* (Pollard et al. 2006).

To establish the robustness of the GABAergic neuron transcriptional profile in developing human neocortex and compare it to mice, we implemented the strategy shown in Fig. 1C. We analyzed 3 additional microarray and RNAseq data sets from GW17-19 human neocortex (Johnson et al. 2009; Miller et al. 2014) (see also http://www.brainspan.org). For each data set, we constructed a series of unsupervised gene coexpression networks, identified the module that was most significantly enriched with markers of human GABAergic neurons (Zeng et al. 2012), and calculated $k_{ME}$ values for every probe/gene with respect to this module.

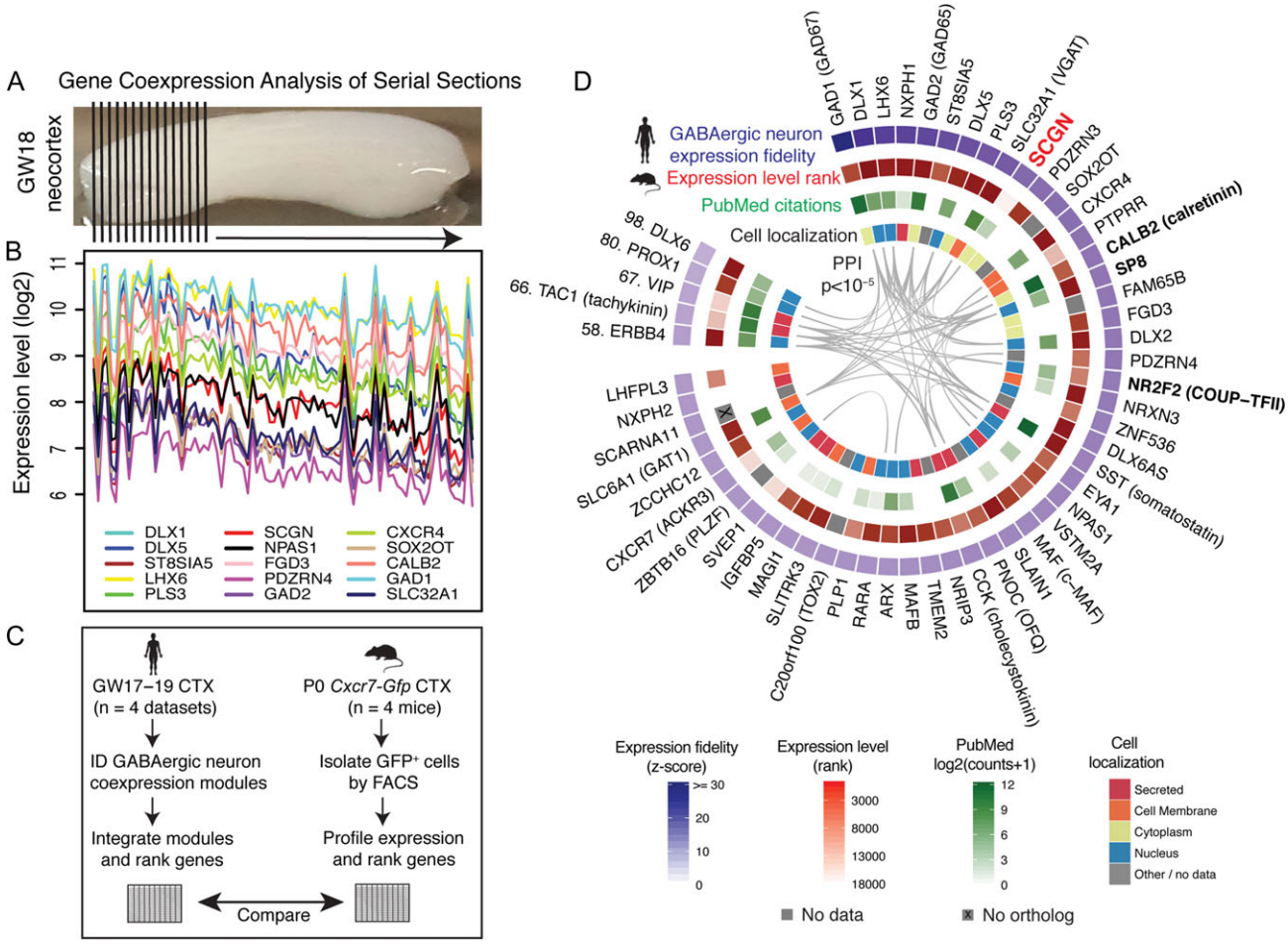


**Figure 1.** GCASS identifies a transcriptional signature of GABAergic neurons in prenatal human neocortex. (*A*) A GW18 human neocortical specimen was analyzed by GCASS ($n = 87$ sections). (*B*) Expression patterns of the top 15 members of the green coexpression module over all sections. (*C*) Schematic of strategy for comparing gene expression in GABAergic neurons between humans and mice. (*D*) Top genes ranked by consensus expression fidelity for GABAergic neurons in GW17-19 human neocortex (blue track). Red track denotes expression level rank in purified GABAergic neurons from P0 *Cxcr7-Gfp* mice. PubMed citations were obtained by queries with gene symbol and "GABAergic" or "interneuron". Cellular localizations are from COMPARTMENTS and PPI are from STRING (Methods).

$k_{ME}$ values for these 4 modules (including the green module from the GCASS data set) were collapsed to unique genes and combined to yield a consensus transcriptional profile of nascent GABAergic neurons. This profile ranks genes by a statistic (z-score), with higher values predicting greater expression fidelity for GABAergic neurons relative to all other cell types in developing human neocortex. This ranking therefore provides an unbiased view of the core transcriptional phenotypes that characterize nascent GABAergic neurons during human corticogenesis. Genes with high z-scores are predicted to encode proteins that are required for the differentiation, migration, and maturation of human GABAergic neurons, including optimal biomarkers. In parallel, we analyzed gene expression in FACS-sorted GABAergic neurons from P0 *Cxcr7-Gfp* transgenic mouse neocortex. *Cxcr7* is coexpressed with *Dlx1*, *Lhx6*, and *Cxcr4* and is required for proper migration of neocortical GABAergic neurons in mice (Wang et al. 2011).

We visualized the top 50 genes in the consensus transcriptional profile of GABAergic neurons in developing human neocortex (plus 5 other known markers that ranked in the top 100), along with their protein–protein interactions (PPI) (Szklarczyk et al. 2015), cellular localizations (Binder et al. 2014), literature citations, and expression level ranks in neocortical GABAergic neurons purified from P0 *Cxcr7-Gfp* transgenic mice (Fig. 1*D*). We observed significantly more PPI than expected by chance and an abundance of nuclear proteins ($n = 18$; Fig. 1*D*), all of which encode transcription factors. Interestingly, many of the genes in Fig. 1*D* had zero or only a handful of literature citations in connection with GABAergic neurons (e.g., *ST8SIA5*, *PLS3*, *PDZRN3*, etc.), highlighting fertile ground for novel molecular studies of interneuron biology.

We examined the genes in Fig. 1*D* and found that most were expressed by mouse GABAergic neurons, suggesting general conservation of transcriptional regulation in these cells between rodents and primates. However, we also identified several genes with evidence for binary expression differences in nascent GABAergic neurons (i.e., ON in human and OFF in mouse), including *SCGN*, *NXPH2*, and *SCARNA11* (Fig. 1*D*). *SCARNA11* is a small nucleolar RNA that localizes to Cajal bodies and has no known orthologue in the mouse genome, whereas *NXPH2* and *SCGN* are protein-coding genes that are present in the mouse genome. We focused on *SCGN*, which ranked in the top 0.03% of all genes in the consensus transcriptional profile of human GABAergic neurons but was expressed at lower levels than >83% of all genes in mouse GABAergic neurons, potentially in the realm of microarray background noise (Fig. 1*D*).

## Secretagogin is Expressed by Postmitotic GABAergic Neurons Derived from the CGE/LGE in Humans but not Mice

*SCGN* encodes a calcium-binding protein that was first discovered as a modifier of insulin release in pancreatic β cells (Wagner et al. 2000). *Scgn* expression has been reported in a variety of neuronal subtypes in mammalian brains (Mulder et al. 2009, 2010) (further reviewed in Alpar et al. 2012), but its cellular origins in prenatal human brain have not been described. Immunofluorescent staining revealed SCGN expression in a large number of cells from the ventricular zone to the pial surface of GW18 human neocortex (Fig. 2*A*). $SCGN^+$ cells exhibited bipolar morphology reminiscent of migrating interneurons and coexpressed multiple markers of GABAergic cells, including SP8, CR, NR2F2 (COUP-TFII), and GABA (Fig. 2*B–J*, Supplementary Figs S2, S3). In contrast, *Scgn* transcript and protein were restricted to ventral regions of the embryonic mouse forebrain and were not detected in neocortex at all time points examined (Fig. 2*K,L*, Supplementary Fig. 4).

Neocortical GABAergic neurons expressing SP8, CR, and NR2F2 are derived mainly from the CGE/LGE of the human subpallium (Reinchisi et al. 2012; Hansen et al. 2013; Ma et al. 2013). We therefore examined whether $SCGN^+$ GABAergic neurons are also derived from these regions in humans. Immunostaining of GW14.5 human telencephalon revealed $SCGN^+$ $SP8^+$ cells throughout the pallium, with a particularly high concentration in the marginal zone (Fig. 3*A–D*). Pallial expression of SCGN was

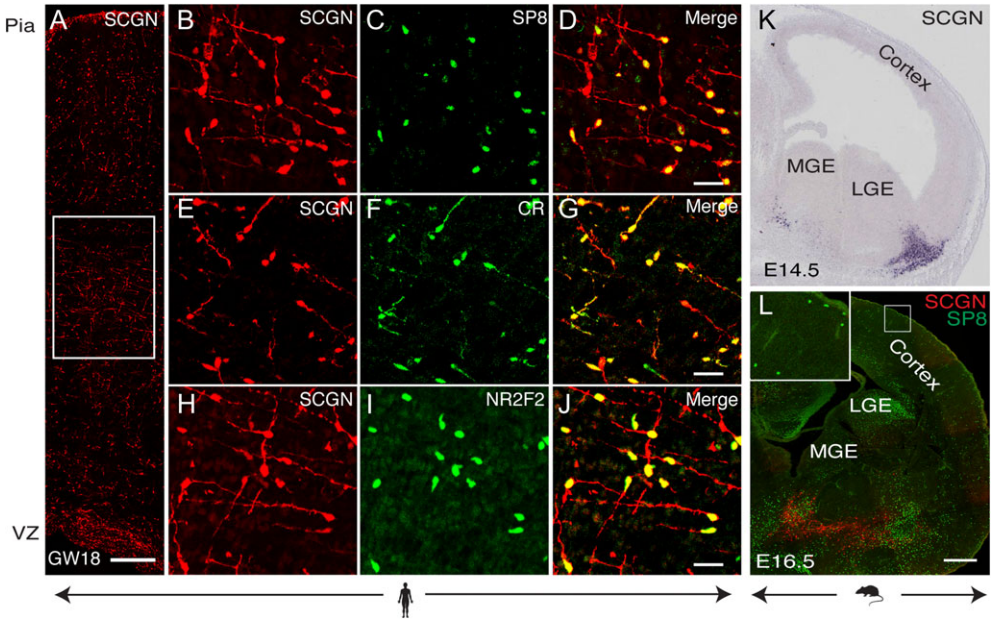


**Figure 2.** Neocortical GABAergic neurons express SCGN during human but not mouse brain development. (*A*) Immunostaining for SCGN in GW18 human neocortex. (*B–J*) Magnified images of boxed area in (*A*) (see Supplementary Fig. 2*F,I,L* for more detailed localization). (*K* and *L*) In situ hybridization for *Scgn* (*K*; http://www.eurexpress.org/ee/) and immunostaining (*L*) for SCGN and SP8 in embryonic mouse brain. Scale bars: 200 μm (*A*, *K*, *L*); 50 μm (*B–J*).

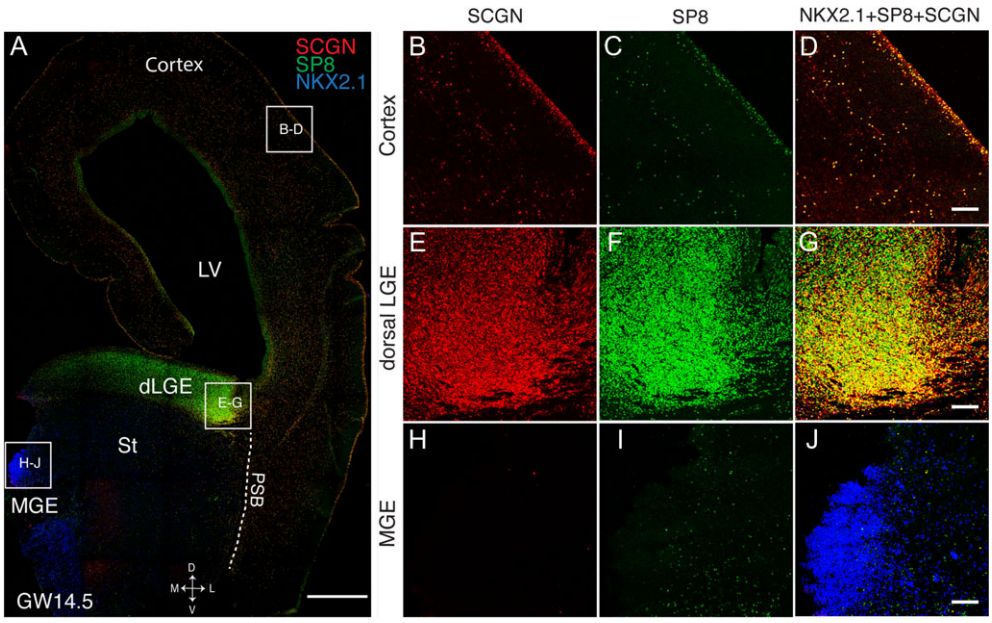


**Figure 3.** SCGN$^+$ GABAergic neurons are highly concentrated in the dLGE and excluded from the MGE in prenatal human brain. (*A*) Coronal section of GW14.5 human telencephalon immunostained for SCGN, SP8, and NKX2.1. LV, lateral ventricle; St, striatum; PSB, pallial–subpallial boundary. (*B–J*) Magnified images of boxed areas in (*A*). Scale bars: 1 mm (*A*); 50 μm (*B–J*).

not observed in glutamatergic neurons, intermediate progenitors, or dividing cells, as evidenced by double immunostaining for TBR1, TBR2, or Ki-67, respectively (Supplementary Fig. 5).

In the subpallium, an extremely dense population of SCGN$^+$ SP8$^+$ cells was present in the dorsal LGE (dLGE) (Fig. 3*A, E–G*). Most of these cells were postmitotic, except for a potential subpopulation near the pallial–subpallial boundary (Supplementary Fig. 5*C*). At GW18, a high density of SCGN$^+$ SP8$^+$ NR2F2$^+$ cells was observed in the CGE and dLGE (Supplementary Fig. 6). In contrast, SCGN was not detected in the MGE (labeled by immunostaining for NKX2.1), despite the presence of some SP8$^+$ cells (Fig. 3*A, H–J*). To confirm these observations, we microdissected GW15 samples from human MGE, LGE, or CGE and cultured them for 4 weeks before immunostaining for SCGN, SP8, and NKX2.1. MGE culture produced cells that were NKX2.1$^+$ SP8$^-$ SCGN$^-$, while LGE and CGE cultures produced cells that were NKX2.1$^-$ SP8$^+$ SCGN$^+$ (Supplementary Fig. 7). Collectively, these results suggest that *SCGN* expression in prenatal human neocortex is restricted to postmitotic GABAergic neurons derived from the CGE/LGE.

To explore whether SCGN expression in nascent neocortical GABAergic neurons is specific to humans, we performed immunostaining of P2 ferret telencephalon (Supplementary Fig. 8). As in humans, we observed no evidence for SCGN$^+$ cells in the MGE. In the LGE, we observed SCGN expression in a subset of SP8$^+$ cells that appeared less extensive than the SCGN$^+$ SP8$^+$ LGE population in humans. Interestingly, we observed a relatively small number of SCGN$^+$ cells in the VZ/SVZ of ferret neocortex, which coexpressed SP8. Therefore, SCGN expression was generally more widespread in the LGE and neocortex of humans compared with ferret at the ages examined.

## Secretagogin Expression in Human Neocortex is Developmentally Regulated and Peaks Before Birth

We next examined *SCGN* expression in human neocortex at later ages. At birth, SCGN was widely expressed in migratory streams of young doublecortin (DCX)$^+$ neurons in the frontal lobe, including neurons comprising the Arc, a newly described caplike structure surrounding the anterior body of the lateral ventricle (Paredes et al. 2016) (Supplementary Fig. 9). These findings are consistent with the idea that the CGE/LGE contribute substantially to late-arriving interneurons in the human frontal lobe (Paredes et al. 2016). Across the human lifespan (Kang et al. 2011), analysis of 11 neocortical areas revealed that *SCGN* expression peaks in the late mid-fetal period (GW21–GW26) and declines monotonically thereafter (Fig. 4A). We confirmed this trend by immunostaining for SCGN in human neocortical samples from 7 months, 6 years, and 24 years. We observed progressively fewer SCGN$^+$ cells over time, with those present in early adulthood enriched in superficial cortical layers (Fig. 4*B–D*). These cells often exhibited bipolar or bitufted morphology and coexpressed CR and VIP (Fig. 4*E–J*), consistent with CGE/LGE origins (Xu et al. 2004; Fogarty et al. 2007; Miyoshi et al. 2010; DeFelipe et al. 2013; Ma et al. 2013; Dzaja et al. 2014; Hladnik et al. 2014).

## Forced Expression of *SCGN* in Mouse GABAergic Neurons Decreases Input Resistance and Increases Total Neurite Length and Arbor Complexity In Vivo

To study the functional consequences of *SCGN* activity in subpallial GABAergic neurons in vivo, we dissociated cells from E14.5 CGE of *Vip-Cre;R26-Ai14* mice and incubated them with either a lenti-*Gfp* or lenti-*Gfp-SCGN* virus. Transduced cells were injected into the visual cortex of P2 host mice and after ~50 days subjected to analysis (Fig. 5A). Because SCGN binds calcium (Wagner et al. 2000), we reasoned that its expression might alter the intrinsic electrophysiological properties of GABAergic neurons. We therefore measured the impact of *SCGN* expression on intrinsic electrophysiological properties through intracellular recordings in acute brain slices from host mice. Compared with transplanted VIP$^+$ neurons expressing

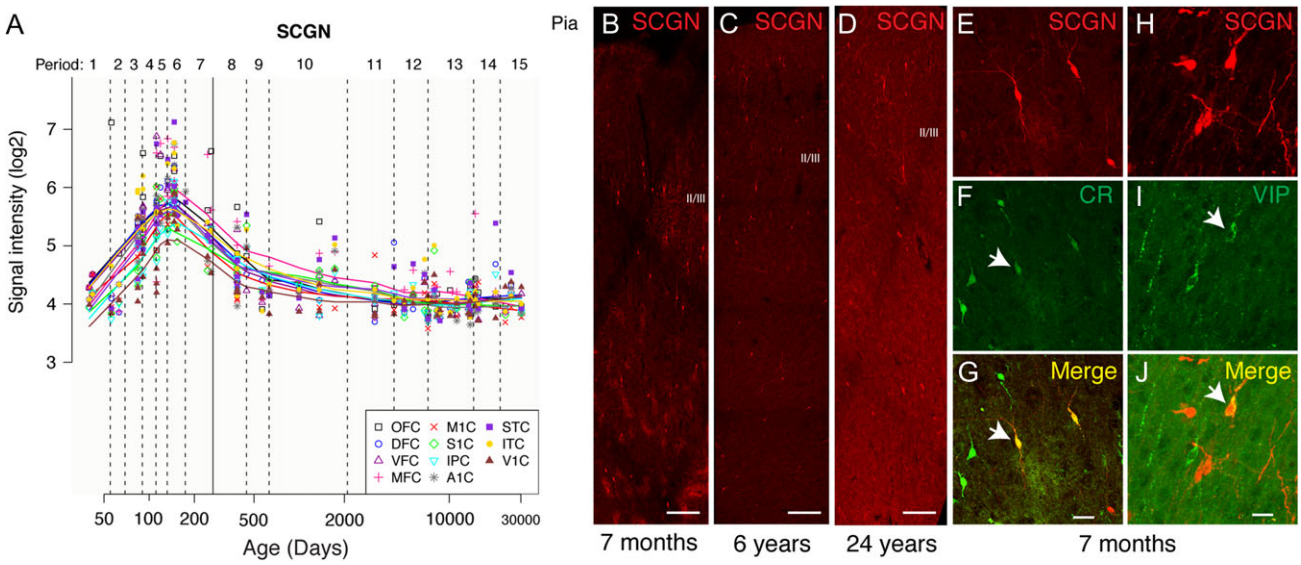


**Figure 4.** Expression of SCGN peaks before birth and preferentially labels interneurons that populate superficial layers of human neocortex. (*A*) Expression patterns in 11 neocortical areas across the human lifespan (Kang et al. 2011) suggest a role for *SCGN* during prenatal brain development (black vertical line denotes birth). (*B–D*) Immunostaining for SCGN in human prefrontal cortex (7 months), superior frontal gyrus (6 years), and entorhinal cortex (24 years). (*E–J*) SCGN$^+$ neurons in human prefrontal cortex (7 months) acquire bipolar/bitufted morphology and coexpress CR and VIP. Scale bars: 150 μm (*B–D*); 50 μm (*E–G*); 30 μm (*H–J*).

lenti-*Gfp*, transplanted VIP$^+$ neurons expressing lenti-*Gfp-SCGN* exhibited a nominally significant decrease in input resistance ($P = 0.02$) and increase in rheobase ($P = 0.025$) (Supplementary Fig. 10). These observations suggest that SCGN$^+$ GABAergic neurons may require increased synaptic input to achieve firing threshold. Because electrical excitability also depends on dendritic geometry (Mainen and Sejnowski 1996; Vetter et al. 2001; Grudt and Perl 2002; Schaefer et al. 2003; Helmstaedter et al. 2009), a corollary to these observations is that *SCGN* expression may alter neuronal morphology. We therefore explored this possibility through morphometric analysis.

Initial observations suggested that *SCGN* expression substantially increased neurite arbor complexity compared with controls (Fig. 5*B*). To study this phenotype more closely, we reconstructed transplanted neurons in 3 dimensions using Neurolucida and confocal microscopy (Fig. 5*C*). We quantified the total neurite length, number of branches, and number of intersections as a function of somal distance via Sholl analysis. SCGN$^+$ neurons exhibited significantly higher values for all of these measures compared with controls (Fig. 5*D–F*). In particular, distal arbor complexity was greatly enhanced (Fig. 5*F*; additional representative neuron tracings are shown in Supplementary Fig. 11). These results suggest that *SCGN* expression in VIP$^+$ mouse GABAergic neurons may affect intrinsic electrophysiological properties by altering neuronal morphology. Furthermore, these findings implicate *SCGN* as the first member of a signaling pathway that contributes to morphological differences between CGE/LGE-derived GABAergic neurons of mice and humans.

## Discussion

This study provides insights into the transcriptional programs that govern GABAergic neuron development in human neocortex and the extent to which they are conserved in mice. Our major findings are as follows: (1) most genes expressed by nascent neocortical GABAergic neurons are conserved between humans and mice; (2) many of these genes have not previously been studied with respect to GABAergic neuron biology; (3) the calcium-binding protein SCGN is robustly expressed by postmitotic GABAergic neurons derived from the CGE/LGE in humans but not mice; and (4) forced expression of *SCGN* in CGE-derived, VIP$^+$ mouse GABAergic neurons dramatically increases total neurite length and arbor complexity in vivo.

Through integrative gene coexpression analysis, we identified many genes that are likely to play conserved yet uncharacterized roles in the differentiation, migration, and maturation of neocortical GABAergic neurons (Fig. 1*D*). These genes include transcription factors such as *ZNF536* and *EYA1*, the first of which falls within one of 108 conservatively defined loci meeting genome-wide significance in association with schizophrenia (Schizophrenia Working Group of the Psychiatric Genomics Consortium 2014). Also present in this list are multiple representatives of distinct protein families, including *NXPH1/NXPH2* and *PDZRN3/PDZRN4*, whose functions in GABAergic neurons are poorly understood. These findings highlight the strength of "guilt-by-association" strategies for revealing novel molecular correlates of cellular identity (Oldham et al. 2008).

The general conservation of transcriptional programs that govern neocortical GABAergic neuron development in humans and mice provides further evidence that the mouse is a defensible model system for studying the potential contributions of these cells to diverse neurological and psychiatric disorders. At the same time, differences in the proportions of GABAergic neuron subtypes between human and mouse neocortex highlight the need for more studies of interneuron development and function using human tissues and cells. For example, interneurons expressing tyrosine hydroxylase appear to be particularly abundant in deep layers of human neocortex relative to other mammalian species (Defelipe 2011). Variation in GABAergic neuron subtype proportions between human and mouse neocortex has also been attributed to species' differences in the neuroanatomical origins of these cells (Letinic et al. 2002; Jakovcevski et al. 2011; Yu and Zecevic 2011; Radonjic et al. 2014a), although this interpretation is not universally accepted (Hansen et al. 2013; Ma et al. 2013). Our finding of molecular differences in SCGN activity between humans

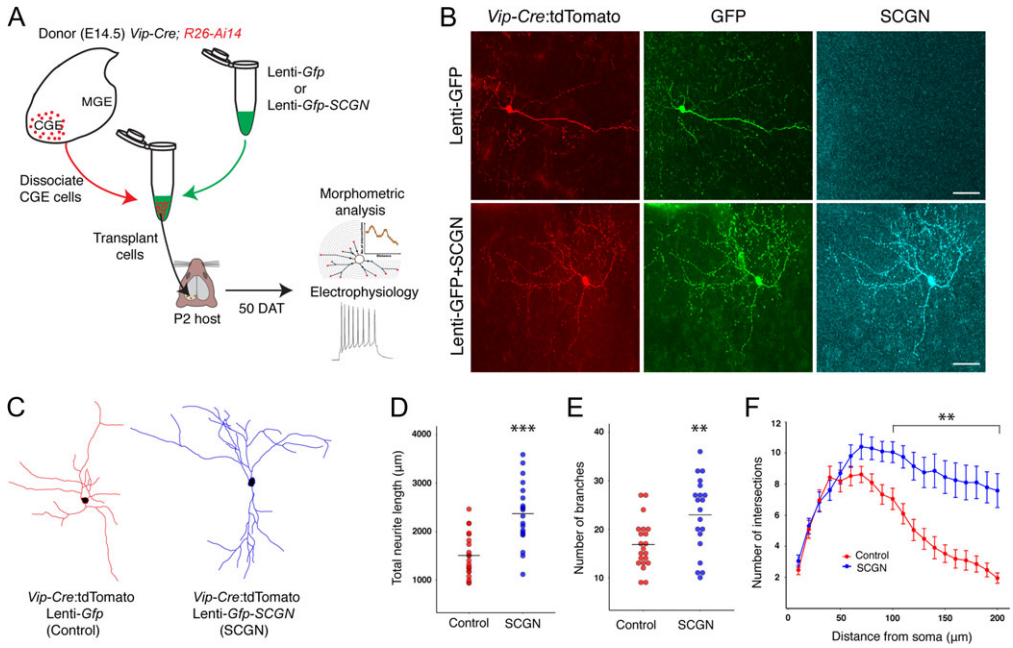


**Figure 5.** Forced expression of *SCGN* increases neurite length and arbor complexity in CGE-derived mouse GABAergic neurons. (*A*) Schematic of transplantation experiment. CGE cells from donor mice expressing tdTomato exclusively in VIP$^+$ neurons (*Vip-Cre; R26-Ai14*) were harvested at E13.5, transduced with lentivirus, and transplanted into P2 recipient visual cortex. (*B*) Cortical sections from recipient mice were immunostained for GFP and SCGN 50 days after transplantation to confirm SCGN expression in transplanted cells. (*C*) Representative Neurolucida reconstructions of transplanted neurons expressing SCGN or empty vector (control). (*D*–*F*) Comparison of total neurite length (*D*), number of branches (*E*), and number of intersections with concentric spheres drawn at 10 μm radius intervals from the soma via Sholl analysis (*F*). *P*-values are from Student's *t*-test (*D*, *E*) and Wilcoxon rank-sum test (*F*; performed separately for each distance): $^{**}P < 0.01$; $^{***}P < 0.001$. Neurolucida tracings are from $n = 21$ (control) and $n = 20$ (SCGN) cells (4 animals per condition, minimum 5 cells per animal). Error bars: one SEM. Scale bars: 50 μm (*B*).

and mice provides further support for efforts to clarify species' differences among subpopulations of GABAergic neurons.

We also note that important categories of evolutionary change are not addressed by our strategy. For example, a gene that is transcribed in human and mouse GABAergic neurons may be expressed at different levels in each species, with important functional consequences. Alternatively, amino-acid substitutions may alter protein function despite comparable gene expression levels. Although there are likely to be many important examples of evolutionary changes affecting brain development that fall into these categories, binary or "Boolean" expression differences represent low-hanging fruit that are comparatively straightforward to identify and test experimentally. For example, we previously used this strategy to identify PDGFD–PDGFRß signaling as a driver of radial glial proliferation during human but not mouse corticogenesis (Lui et al. 2014).

To our knowledge, *SCGN* represents the first example of a gene whose expression distinguishes neocortical GABAergic neurons of humans and mice during brain development. Interestingly, phylogenetic differences in *Scgn* expression have previously been reported for other subtypes of telencephalic neurons. For example, a recent study identified a subpopulation of parvalbumin$^+$ interneurons that coexpress *Scgn* in the dorsal striatum of rats, but not mice (Garas et al. 2016). Another group has found that in gray mouse lemurs—but not in mice—*Scgn* is expressed by cholinergic neurons in embryonic basal forebrain and neuroblasts in the rostral migratory stream (Mulder et al. 2009; Mulder et al. 2010). The evolutionary variability in neuronal expression patterns of *Scgn* appears to contrast with other calcium-binding proteins such as CR and calbindin (which are generally thought to label orthologous cell types in mammalian brains), despite the fact that SCGN shares a high degree of sequence homology with these proteins (Alpar et al. 2012).

Phylogenetic differences in neuronal expression patterns of *Scgn* suggest that its functions have diverged from related calcium-binding proteins. There is support for this idea from biochemical studies. Previous work has shown that the calcium affinity of SCGN is far lower than traditional calcium buffers such as CR and calbindin, and comparable to that of synaptotagmin I (Rogstam et al. 2007). Like synaptotagmin I, SCGN undergoes a conformational change upon binding calcium that potentiates physical interaction with the t-snare protein SNAP25 (Rogstam et al. 2007). These observations suggest that SCGN is involved in calcium-dependent exocytosis, which is consistent with its ability to modulate insulin release in the pancreas (Wagner et al. 2000) and corticotropin-releasing hormone release in the hypothalamus (Romanov et al. 2015). We therefore propose that *SCGN* expression in CGE/LGE-derived GABAergic neurons increases neurite length and arbor complexity by promoting calcium-dependent exocytosis of plasmalemmal precursor vesicles in growth cones. Future studies will explore this possibility and whether such vesicles contain unidentified signaling molecules that may amplify these effects in an autocrine/paracrine fashion.

Others have observed that *Scgn* appears to be preferentially expressed by non-differentiated neurons in primate brains (Alpar et al. 2012). These observations suggest that *Scgn* expression may provide a general mechanism for increasing neurite length and arbor complexity in diverse neuronal subtypes with varied morphologies. In the case of horse-tail GABAergic

neurons in primate neocortex, SCGN activity may provide the "raw material" necessary for the long, vertically oriented axon collaterals and dendritic branches that characterize these cells, whose mature morphologies likely depend on other factors. In this regard, it will be interesting to explore potential synergies between *SCGN* and *NXPH2*, which encodes a secreted glycoprotein that serves as a ligand to the α-neurexin family of transsynaptic cell adhesion molecules (Petrenko et al. 1996; Missler and Sudhof 1998).

Beyond the cell-intrinsic effects of *SCGN* expression on neuronal morphology, it is also important to recognize that GABA signaling provides excitatory drive for immature neocortical networks and has been implicated in most aspects of corticogenesis, including proliferation, migration, and synaptogenesis (Wang and Kriegstein 2009). Because SCGN expression in human neocortex is widespread by GW14.5 (Fig. 3), when deep cortical layers are still being formed, it is spatiotemporally well-positioned to expand the ability of CGE/LGE-derived GABAergic neurons to coordinate diverse aspects of neocortical development.

## Supplementary Material

Supplementary data is available at *Cerebral Cortex* online.

## Funding

The UCSF Program for Breakthrough Biomedical Research, which is funded in part by the Sandler Foundation, and a Scholar Award from the UCSF Weill Institute for Neurosciences (M.C.O.); post-doctoral grants from the Wenner-Gren Foundation and Hjärnfonden (C.S.R.); the National Institutes of Health (P01 NS083513) along with a generous gift from the John G. Bowes Research Fund (A.A.B.). A.A.B. is the Heather and Melanie Muss Endowed Chair and Professor of Neurological Surgery at UCSF.

## Notes

We thank the staff at San Francisco General Hospital Women's Options Center for providing access to donated human prenatal tissue. We thank Joe DeYoung and staff at the UCLA Neurogenomics Core facility for microarray data generation and Caitlyn Gertz for the gift of ferret tissue. Due to space limitations, we apologize that many primary and historical publications have not been cited. *Conflict of Interest*: C.R.N., A.R.K., A.A.B., and J.L.R. are co-founders of Neurona Therapeutics. C.R.N. and J.S. are employees of Neurona Therapeutics. C.R.N., J.S., A.R.K., A.A.B., and J.L.R. own shares in the company.

## REFERENCES

Al-Jaberi N, Lindsay S, Sarma S, Bayatti N, Clowry GJ. 2015. The early fetal development of human neocortical GABAergic interneurons. Cereb Cortex. 25:631–645.

Alpar A, Attems J, Mulder J, Hokfelt T, Harkany T. 2012. The renaissance of Ca2+-binding proteins in the nervous system: secretagogin takes center stage. Cell Signal. 24:378–387.

Barbosa-Morais NL, Dunning MJ, Samarajiwa SA, Darot JF, Ritchie ME, Lynch AG, Tavare S. 2010. A re-annotation pipeline for Illumina BeadArrays: improving the interpretation of gene expression data. Nucleic Acids Res. 38:e17.

Barinka F, Magloczky Z, Zecevic N. 2015. Editorial: at the top of the interneuronal pyramid-calretinin expressing cortical interneurons. Front Neuroanat. 9:108.

Bayatti N, Moss JA, Sun L, Ambrose P, Ward JF, Lindsay S, Clowry GJ. 2008. A molecular neuroanatomical study of the developing human neocortex from 8 to 17 postconceptional weeks revealing the early differentiation of the subplate and subventricular zone. Cereb Cortex. 18:1536–1548.

Beaulieu C. 1993. Numerical data on neocortical neurons in adult rat, with special reference to the GABA population. Brain Res. 609:284–292.

Beaulieu C, Campistron G, Crevier C. 1994. Quantitative aspects of the GABA circuitry in the primary visual cortex of the adult rat. J Comp Neurol. 339:559–572.

Beaulieu C, Kisvarday Z, Somogyi P, Cynader M, Cowey A. 1992. Quantitative distribution of GABA-immunopositive and -immunonegative neurons and synapses in the monkey striate cortex (area 17). Cereb Cortex. 2:295–309.

Binder JX, Pletscher-Frankild S, Tsafou K, Stolte C, O'Donoghue SI, Schneider R, Jensen LJ. 2014. COMPARTMENTS: unification and visualization of protein subcellular localization evidence. Database (Oxford). 2014:bau012.

Bolstad BM, Irizarry RA, Astrand M, Speed TP. 2003. A comparison of normalization methods for high density oligonucleotide array data based on variance and bias. Bioinformatics. 19:185–193.

Cajal SR. 1899. Apuntes para el studio estructural de la corteza visual del cerebro humano. Rev Ibero-Americana Cienc Med. 1:1–14.

Cajal SR. 1923. Recuerdos de mi vida: Historia de mi labor científica. Madrid, Spain: Alianza Editorial.

Clowry G, Molnar Z, Rakic P. 2010. Renewed focus on the developing human neocortex. J Anat. 217:276–288.

Defelipe J. 2011. The evolution of the brain, the human nature of cortical circuits, and intellectual creativity. Front Neuroanat. 5:29.

DeFelipe J, Ballesteros-Yanez I, Inda MC, Munoz A. 2006. Double-bouquet cells in the monkey and human cerebral cortex with special reference to areas 17 and 18. Prog Brain Res. 154:15–32.

DeFelipe J, Lopez-Cruz PL, Benavides-Piccione R, Bielza C, Larranaga P, Anderson S, Burkhalter A, Cauli B, Fairen A, Feldmeyer D, et al. 2013. New insights into the classification and nomenclature of cortical GABAergic interneurons. Nat Rev Neurosci. 14:202–216.

del Rio MR, DeFelipe J. 1996. Colocalization of calbindin D-28k, calretinin, and GABA immunoreactivities in neurons of the human temporal cortex. J Comp Neurol. 369:472–482.

Dzaja D, Hladnik A, Bicanic I, Bakovic M, Petanjek Z. 2014. Neocortical calretinin neurons in primates: increase in proportion and microcircuitry structure. Front Neuroanat. 8:103.

Fisher RA. 1970. Statistical methods for research workers. In: Davien. CT: Hafner Publishing Company.

Fitzpatrick D, Lund JS, Schmechel DE, Towles AC. 1987. Distribution of GABAergic neurons and axon terminals in the macaque striate cortex. J Comp Neurol. 264:73–91.

Fogarty M, Grist M, Gelman D, Marin O, Pachnis V, Kessaris N. 2007. Spatial genetic patterning of the embryonic neuroepithelium generates GABAergic interneuron diversity in the adult cortex. J Neurosci. 27:10935–10946.

Gabbott PL, Bacon SJ. 1996. Local circuit neurons in the medial prefrontal cortex (areas 24a,b,c, 25 and 32) in the monkey: I. Cell morphology and morphometrics. J Comp Neurol. 364:567–608.

Gabbott PL, Dickie BG, Vaid RR, Headlam AJ, Bacon SJ. 1997. Local-circuit neurones in the medial prefrontal cortex (areas 25, 32 and 24b) in the rat: morphology and quantitative distribution. J Comp Neurol. 377:465–499.

Garas FN, Shah RS, Kormann E, Doig NM, Vinciati F, Nakamura KC, Dorst MC, Smith Y, Magill PJ, Sharott A. 2016. Secretagogin expression delineates functionally-specialized populations of striatal parvalbumin-containing interneurons. eLife. 5:e16088.

Grudt TJ, Perl ER. 2002. Correlations between neuronal morphology and electrophysiological features in the rodent superficial dorsal horn. J Physiol. 540:189–207.

Hansen DV, Lui JH, Flandin P, Yoshikawa K, Rubenstein JL, Alvarez-Buylla A, Kriegstein AR. 2013. Non-epithelial stem cells and cortical interneuron production in the human ganglionic eminences. Nat Neurosci. 16:1576–1587.

Hansen DV, Lui JH, Parker PR, Kriegstein AR. 2010. Neurogenic radial glia in the outer subventricular zone of human neocortex. Nature. 464:554–561.

Helmstaedter M, Sakmann B, Feldmeyer D. 2009. The relation between dendritic geometry, electrical excitability, and axonal projections of L2/3 interneurons in rat barrel cortex. Cereb Cortex. 19:938–950.

Hendry SH, Schwark HD, Jones EG, Yan J. 1987. Numbers and proportions of GABA-immunoreactive neurons in different areas of monkey cerebral cortex. J Neurosci. 7:1503–1519.

Hladnik A, Dzaja D, Darmopil S, Jovanov-Milosevic N, Petanjek Z. 2014. Spatio-temporal extension in site of origin for cortical calretinin neurons in primates. Front Neuroanat. 8:50.

Hornung JP, De Tribolet N. 1994. Distribution of GABA-containing neurons in human frontal cortex: a quantitative immunocytochemical study. Anat Embryol (Berl). 189: 139–145.

Jakovcevski I, Mayer N, Zecevic N. 2011. Multiple origins of human neocortical interneurons are supported by distinct expression of transcription factors. Cereb Cortex. 21: 1771–1782.

Johnson MB, Kawasawa YI, Mason CE, Krsnik Z, Coppola G, Bogdanovic D, Geschwind DH, Mane SM, State MW, Sestan N. 2009. Functional and evolutionary insights into human brain development through global transcriptome analysis. Neuron. 62:494–509.

Johnson WE, Li C, Rabinovic A. 2007. Adjusting batch effects in microarray expression data using empirical Bayes methods. Biostatistics. 8:118–127.

Jones EG. 2009. The origins of cortical interneurons: mouse versus monkey and human. Cereb Cortex. 19:1953–1956.

Jones EG, Huntley GW, Benson DL. 1994. Alpha calcium/calmodulin-dependent protein kinase II selectively expressed in a subpopulation of excitatory neurons in monkey sensory-motor cortex: comparison with GAD-67 expression. J Neurosci. 14:611–629.

Jones EG, Peters A. 1984. Cerebral cortex. In: Cellular Components of the Cerebral Cortex. Volume 1. New York: Plenum Press.

Kang HJ, Kawasawa YI, Cheng F, Zhu Y, Xu X, Li M, Sousa AM, Pletikos M, Meyer KA, Sedmak G, et al. 2011. Spatio-temporal transcriptome of the human brain. Nature. 478: 483–489.

Langfelder P, Horvath S. 2008. WGCNA: an R package for weighted correlation network analysis. BMC Bioinformatics. 9:559.

Larimer P, Spatazza J, Espinosa JS, Tang Y, Kaneko M, Hasenstaub AR, Stryker MP, Alvarez-Buylla A. 2016. Caudal ganglionic eminence precursor transplants disperse and integrate as lineage-specific interneurons but do not induce cortical plasticity. Cell Rep. 16:1391–1404.

Letinic K, Zoncu R, Rakic P. 2002. Origin of GABAergic neurons in the human neocortex. Nature. 417:645–649.

Lin CS, Lu SM, Schmechel DE. 1986. Glutamic acid decarboxylase and somatostatin immunoreactivities in rat visual cortex. J Comp Neurol. 244:369–383.

Lui JH, Nowakowski TJ, Pollen AA, Javaherian A, Kriegstein AR, Oldham MC. 2014. Radial glia require PDGFD-PDGFRbeta signalling in human but not mouse neocortex. Nature. 515: 264–268.

Ma T, Wang C, Wang L, Zhou X, Tian M, Zhang Q, Zhang Y, Li J, Liu Z, Cai Y, et al. 2013. Subcortical origins of human and monkey neocortical interneurons. Nat Neurosci. 16:1588–1597.

Mainen ZF, Sejnowski TJ. 1996. Influence of dendritic structure on firing pattern in model neocortical neurons. Nature. 382: 363–366.

Marin O. 2012. Interneuron dysfunction in psychiatric disorders. Nat Rev Neurosci. 13:107–120.

Meinecke DL, Peters A. 1987. GABA immunoreactive neurons in rat visual cortex. J Comp Neurol. 261:388–404.

Micheva KD, Beaulieu C. 1995. Postnatal development of GABA neurons in the rat somatosensory barrel cortex: a quantitative study. Eur J Neurosci. 7:419–430.

Miller JA, Ding SL, Sunkin SM, Smith KA, Ng L, Szafer A, Ebbert A, Riley ZL, Royall JJ, Aiona K, et al. 2014. Transcriptional landscape of the prenatal human brain. Nature. 508:199–206.

Missler M, Sudhof TC. 1998. Neurexophilins form a conserved family of neuropeptide-like glycoproteins. J Neurosci. 18: 3630–3638.

Miyoshi G, Hjerling-Leffler J, Karayannis T, Sousa VH, Butt SJ, Battiste J, Johnson JE, Machold RP, Fishell G. 2010. Genetic fate mapping reveals that the caudal ganglionic eminence produces a large and diverse population of superficial cortical interneurons. J Neurosci. 30:1582–1594.

Molnar Z, Clowry G. 2012. Cerebral cortical development in rodents and primates. Prog Brain Res. 195:45–70.

Mulder J, Spence L, Tortoriello G, Dinieri JA, Uhlen M, Shui B, Kotlikoff MI, Yanagawa Y, Aujard F, Hokfelt T, et al. 2010. Secretagogin is a Ca2+-binding protein identifying prospective extended amygdala neurons in the developing mammalian telencephalon. Eur J Neurosci. 31:2166–2177.

Mulder J, Zilberter M, Spence L, Tortoriello G, Uhlen M, Yanagawa Y, Aujard F, Hokfelt T, Harkany T. 2009. Secretagogin is a Ca2+-binding protein specifying subpopulations of telencephalic neurons. Proc Natl Acad Sci U S A. 106:22492–22497.

Oldham MC, Konopka G, Iwamoto K, Langfelder P, Kato T, Horvath S, Geschwind DH. 2008. Functional organization of the transcriptome in human brain. Nat Neurosci. 11: 1271–1282.

Oldham MC, Langfelder P, Horvath S. 2012. Network methods for describing sample relationships in genomic datasets: application to Huntington's disease. BMC Syst Biol. 6:63.

Paredes MF, James D, Gil-Perotin S, Kim H, Cotter JA, Ng C, Sandoval K, Rowitch DH, Xu D, McQuillen PS, et al. 2016. Extensive migration of young neurons into the infant human frontal lobe. Science. 354 (6308):aaf7073.

Petrenko AG, Ullrich B, Missler M, Krasnoperov V, Rosahl TW, Sudhof TC. 1996. Structure and evolution of neurexophilin. J Neurosci. 16:4360–4369.

Pollard KS, Salama SR, Lambert N, Lambot MA, Coppens S, Pedersen JS, Katzman S, King B, Onodera C, Siepel A, et al. 2006. An RNA gene expressed during cortical development evolved rapidly in humans. Nature. 443:167–172.

Radonjic NV, Ayoub AE, Memi F, Yu X, Maroof A, Jakovcevski I, Anderson SA, Rakic P, Zecevic N. 2014a. Diversity of cortical interneurons in primates: the role of the dorsal proliferative niche. Cell Rep. 9:2139–2151.

Radonjic NV, Ortega JA, Memi F, Dionne K, Jakovcevski I, Zecevic N. 2014b. The complexity of the calretinin-expressing progenitors in the human cerebral cortex. Front Neuroanat. 8:82.

Reinchisi G, Ijichi K, Glidden N, Jakovcevski I, Zecevic N. 2012. COUP-TFII expressing interneurons in human fetal forebrain. Cereb Cortex. 22:2820–2830.

Ren JQ, Aika Y, Heizmann CW, Kosaka T. 1992. Quantitative analysis of neurons and glial cells in the rat somatosensory cortex, with special reference to GABAergic neurons and parvalbumin-containing neurons. Exp Brain Res. 92:1–14.

Rogstam A, Linse S, Lindqvist A, James P, Wagner L, Berggard T. 2007. Binding of calcium ions and SNAP-25 to the hexa EF-hand protein secretagogin. Biochem J. 401:353–363.

Romanov RA, Alpar A, Zhang MD, Zeisel A, Calas A, Landry M, Fuszard M, Shirran SL, Schnell R, Dobolyi A, et al. 2015. A secretagogin locus of the mammalian hypothalamus controls stress hormone release. EMBO J. 34:36–54.

Santana N, Bortolozzi A, Serrats J, Mengod G, Artigas F. 2004. Expression of serotonin1A and serotonin2A receptors in pyramidal and GABAergic neurons of the rat prefrontal cortex. Cereb Cortex. 14:1100–1109.

Schaefer AT, Larkum ME, Sakmann B, Roth A. 2003. Coincidence detection in pyramidal neurons is tuned by their dendritic branching pattern. J Neurophysiol. 89:3143–3154.

Schizophrenia Working Group of the Psychiatric Genomics Consortium. 2014. Biological insights from 108 schizophrenia-associated genetic loci. Nature. 511:421–427.

Southwell DG, Nicholas CR, Basbaum AI, Stryker MP, Kriegstein AR, Rubenstein JL, Alvarez-Buylla A. 2014. Interneurons from embryonic development to cell-based therapy. Science. 344:1240622.

Szklarczyk D, Franceschini A, Wyder S, Forslund K, Heller D, Huerta-Cepas J, Simonovic M, Roth A, Santos A, Tsafou KP, et al. 2015. STRING v10: protein-protein interaction networks, integrated over the tree of life. Nucleic Acids Res. 43: D447–D452.

Tamamaki N, Yanagawa Y, Tomioka R, Miyazaki J, Obata K, Kaneko T. 2003. Green fluorescent protein expression and colocalization with calretinin, parvalbumin, and somatostatin in the GAD67-GFP knock-in mouse. J Comp Neurol. 467:60–79.

Vetter P, Roth A, Hausser M. 2001. Propagation of action potentials in dendrites depends on dendritic morphology. J Neurophysiol. 85:926–937.

Wagner L, Oliyarnyk O, Gartner W, Nowotny P, Groeger M, Kaserer K, Waldhausl W, Pasternack MS. 2000. Cloning and expression of secretagogin, a novel neuroendocrine- and pancreatic islet of Langerhans-specific Ca2+-binding protein. J Biol Chem. 275:24740–24751.

Wang DD, Kriegstein AR. 2009. Defining the role of GABA in cortical development. J Physiol. 587:1873–1879.

Wang Y, Li G, Stanco A, Long JE, Crawford D, Potter GB, Pleasure SJ, Behrens T, Rubenstein JL. 2011. CXCR4 and CXCR7 have distinct functions in regulating interneuron migration. Neuron. 69:61–76.

Xu Q, Cobos I, De La Cruz E, Rubenstein JL, Anderson SA. 2004. Origins of cortical interneuron subtypes. J Neurosci. 24: 2612–2622.

Yanez IB, Munoz A, Contreras J, Gonzalez J, Rodriguez-Veiga E, DeFelipe J. 2005. Double bouquet cell in the human cerebral cortex and a comparison with other mammals. J Comp Neurol. 486:344–360.

Yu X, Zecevic N. 2011. Dorsal radial glial cells have the potential to generate cortical interneurons in human but not in mouse brain. J Neurosci. 31:2413–2420.

Zeng H, Shen EH, Hohmann JG, Oh SW, Bernard A, Royall JJ, Glattfelder KJ, Sunkin SM, Morris JA, Guillozet-Bongaarts AL, et al. 2012. Large-scale cellular-resolution gene profiling in human neocortex reveals species-specific molecular signatures. Cell. 149:483–496.